



## Process of cracking in reinforced concrete beams (simulation and experiment)

I. N. Shardakov, A. P. Shestakov, I.O. Glot

*Institute of Continuous Media Mechanics of the Ural Branch of Russian Academy of Science (ICMM UB RAS), Korolev str., 1, Perm, 614013, Russia.*

*shardakov@icmm.ru, shap@icmm.ru, glot@icmm.ru*

A.A. Bykov

*Perm National Research Polytechnic University, Komsomolsky ave., 29, Perm, 614990, Russia*

*violentbarpy@ya.ru*

**ABSTRACT.** The paper presents the results of experimental and theoretical investigations of the mechanisms of crack formation in reinforced concrete beams subjected to quasi-static bending. The boundary-value problem has been formulated in the framework of brittle fracture mechanics and solved using the finite-element method. Numerical simulation of the vibrations of an uncracked beam and a beam with cracks of different size serves to determine the pattern of changes in the spectrum of eigenfrequencies observed during crack evolution. A series of sequential quasi-static 4-point bend tests leading to the formation of cracks in a reinforced concrete beam were performed. At each loading step, the beam was subjected to an impulse load to induce vibrations. Two stages of cracking were detected. During the first stage the nonconservative process of deformation begins to develop, but has not visible signs. The second stage is an active cracking, which is marked by a sharp change in eigenfrequencies. The boundary of a transition from one stage to another is well registered. The vibration behavior was examined for the ordinary concrete beams and the beams strengthened with a carbon-fiber polymer. The obtained results show that the vibrodiagnostic approach is an effective tool for monitoring crack formation and assessing the quality of measures aimed at strengthening concrete structures.

**KEYWORDS.** Reinforced concrete; Crack nucleation; Vibrodiagnostics; Experiment; Mathematical modeling.



**Citation:** Shardakov, I. N., Bykov, A.A., Shestakov, A. P., Glot, I.O., Process of cracking in reinforced concrete beams (simulation and experiment), *Frattura ed Integrità Strutturale*, 38 (2016) 339-350.

**Received:** 02.06.2016

**Accepted:** 30.08.2016

**Published:** 01.10.2016

**Copyright:** © 2016 This is an open access article under the terms of the CC-BY 4.0, which permits unrestricted use, distribution, and reproduction in any medium, provided the original author and source are credited.

### INTRODUCTION

Reinforced concrete structures have found wide application in the construction industry. Like other construction materials, reinforced concrete has limited strength characteristics. When these limiting values are exceeded, the structure may fail. Fracture of concrete usually occurs as the process of nucleation and growth of cracks. Initially

the crack formation does not lead to complete loss of the carrying capacity of the structure, but it can be considered as a fracture precursor. Knowledge of the crack nucleation process is important to ensure early prediction of emergency situations and prompt use of techniques to restore damaged reinforced concrete structures.

Nowadays, there are many ways to monitor cracks in concrete structures. Common visual observation methods are helpful in the evaluation of big visible damages, while the hidden or inaccessible defects cannot be identified. The local methods of inspection are actively used as well. They involve recording various physical quantities, such as ultrasonic waves [1], eddy currents [2], temperature fields [3], acoustic emission [4], X-ray, magnetic particles [5], and so on. A survey of nondestructive testing methods applied to reinforced concrete structures can be found in [6]. These methods also have some limitations: one should know a priori the region with defects or use many transducers; the region where a defect may appear should be accessible for examination. The location of a defect may remain unexamined because only a small part of the structure can be examined with these methods. Most local methods are rather expensive, and it takes much time to investigate the structure using these techniques. The methods for crack detection and pattern recognition based on image processing are described in [7].

Another direction in flaw detection technology includes global methods aimed at discovering damage via the assessment of the mechanical behavior of the entire structure. The main advantage of such methods is that they do not require a great number of transducers to be located in close proximity to defects. Most commonly used and promising global methods of nondestructive testing are vibration approaches [8]. They are based on the fact that the variations of physical properties (mass, rigidity, damping) of an object cause the changes in modal parameters, which qualitatively and quantitatively characterize natural vibrations. A survey of vibration approaches is provided in [9-11], and their applications to reinforced concrete structures are described in [12]. Vibration nondestructive testing methods employ various modal parameters. The analysis of eigenfrequencies allowing early damage detection is given in [13]. Damage localization problems have been solved by using a criterion based on the comparison of two mode shapes in damaged and undamaged states [14]. Information about the curvature of eigenmode shapes serves as an indicator of defects in beam structures [15]. Data on eigenmode shape deformation energy have been used for damage localization in [16]. A method for estimating the state of bridges, which is based on the information regarding a compliance matrix, is described in [17]. In connection with the vibration methods of study of quasi-brittle materials destruction the works [18-20] should be noted where the methods of wavelet analysis are successfully used to identify the fracture process.

In the present paper, we propose a new variant of the vibration method to detect the crack location and crack opening degree by analyzing the changes in the eigenfrequencies spectrum associated with the occurrence of cracks. The method allows us to perform monitoring the strain state of structures, where the region of most probable fracture is known, but free access to it is absent.

## **MATHEMATICAL MODEL OF DEFORMATION PROCESSES IN REINFORCED STRUCTURE**

The stress-strain state of reinforced concrete beams under quasi-static four-point bending is studied. The beam is reinforced by two plane steel frameworks joined together by vertical elements. The structural scheme and characteristic sizes of the beam are shown in Fig. 1 (a). At a certain stage of the loading, cracking starts in the beam. Works [21, 22] focus on the mathematical modeling of this process and comparing the simulation results and experimental data.

The proposed approach is based on the analysis of vibrations of a reinforced concrete beam that occur in response to impact loads applied to a certain part of the beam. Comparison of the vibration response of a solid beam and a beam having different-size cracks makes it possible:

- to evaluate the sensitivity of spectral properties of a reinforced concrete beam to crack nucleation and growth;
- to find pulse load, causing vibrations with eigenfrequencies most sensitive to cracking and to define load parameters;
- to identify patterns of change in eigenfrequencies associated with the emergence and growth of cracks.

A calculation scheme for the problem of vibrations of a reinforced beam having a crack is given in Fig. 1 (b). A crack that occurs in concrete is represented as a volume  $V_2$  occupied by the material exhibiting practically zero mechanical properties. This approach is valid for cracks called opening mode cracks. It is precisely these cracks that appear in the beam tested under four-point bending conditions used in our experiment. As regards other types of cracks, having no gap between the edges of the crack, it is necessary to consider the interaction between the opposite surfaces of the crack, taking into account the dissipation of mechanical energy. Our approach can be adapted for these types of cracks.

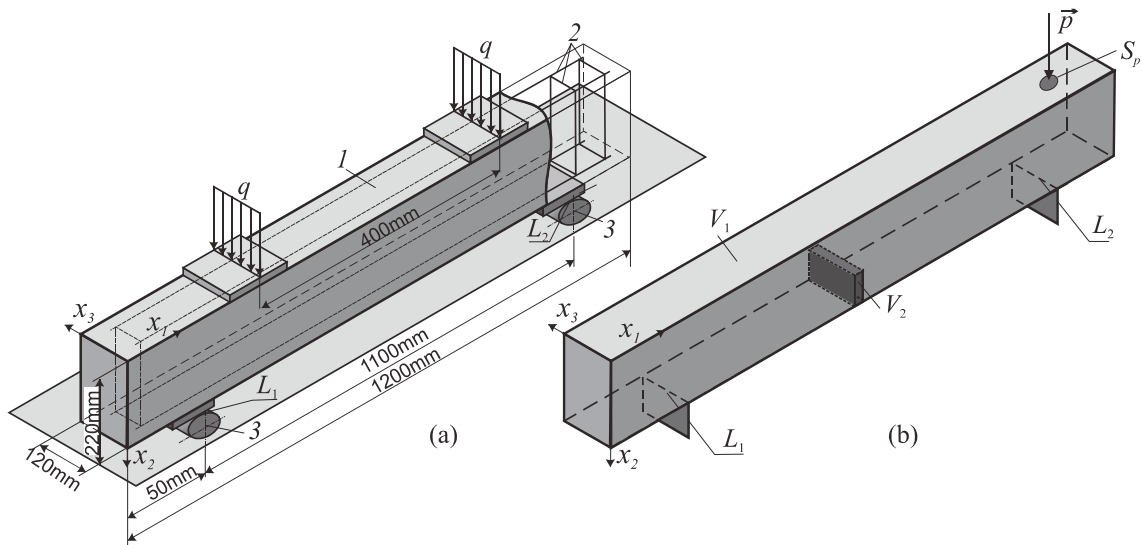


Figure 1: Four-point bending of reinforced concrete beam (a) and the calculation scheme of the beam with a crack (b).

According to Fig. 1, the developed mathematical model describes all structural elements of the beam: concrete (1), steel reinforcement (2), and supporting elements (3).

The problem is formulated by using the virtual displacement principle [23].

$$\delta A_\sigma^b + \delta A_\sigma^o + \delta A_\sigma^a = \delta A_f^b + \delta A_f^o + \delta A_f^a. \quad (1)$$

Boundary and initial conditions are specified as

$$\begin{aligned} u_1 = u_2 = u_3 = 0, \quad \mathbf{x} \in L_1; \quad u_2 = u_3 = 0, \quad \mathbf{x} \in L_2 \\ u_i|_{t=0} = 0, \quad \partial u_i / \partial t|_{t=0} = 0, \quad i \in \overline{1, 3}; \quad x \in V_1 \cup V_2 \\ \mathbf{n} \cdot \boldsymbol{\sigma} \cdot \mathbf{n} = p_n(t), \quad x \in S_p \end{aligned} \quad (2)$$

Boundary conditions imposed on free surfaces, contact lines between the beam and supporting elements and boundary between the steel reinforcement and concrete follow from the variational Eq. (1).

The variation of the work of internal and external forces for the structural elements of the beam can be written as:

$$\begin{aligned} \delta A_\sigma^k &= \int_{V^b} \sigma_{ij}^k \cdot \delta \varepsilon_{ij}^k dV \\ \delta A_f^k &= - \int_{V^b} \rho^k \frac{\partial^2 u_i^k}{\partial t^2} \delta u_i^k dV + \int_{S_p^b} p_i^k \delta u_i^k dS \end{aligned} \quad (3)$$

Expressions (1)-(3) contain the following notation:  $\delta A_\sigma$  – variation of the work of internal forces;  $\delta A_f$  – variation of the work of inertia and external forces; the superscripts  $b, o, a$  denote concrete, supporting elements and a reinforcement rods, respectively, the upper index  $k$  is used as “ $b$ ” “ $a$ ” and “ $o$ ” for different structural elements,  $i, j$  – integer indices taking values 1, 2, 3 in accordance with the axes of Cartesian coordinate system  $(x_1, x_2, x_3)$ ;  $u_i^k$  – displacement vector components;  $\varepsilon_{ij}^k$ ,  $\sigma_{ij}^k$  – strain and stress tensor components;  $\rho^k$  – material density;  $p_i^k$  – components of the external force vector describing the impulse force applied along the normal  $n$  to the localized surface areas  $S_p$  of the beam.

The strain tensor components  $\varepsilon_{ij}^k$  are determined by the relations:

$$\varepsilon_{ij}^k = \frac{1}{2} \left( \frac{\partial u_i^b}{\partial x_j} + \frac{\partial u_j^b}{\partial x_i} \right) \quad (4)$$

According to the Hooke's law, the stress tensor components  $\sigma_{ij}^k$  are written as:

$$\sigma_{ij}^k = \frac{E^k}{1+\nu^b} \varepsilon_{ij}^k + \frac{E^k \nu^k}{(1+\nu^b)(1-2\nu^b)} \varepsilon_{kk}^k \delta_{ij} \quad (5)$$

Tab. 1 summarizes the physical properties of materials of the structural elements of the beam.

Structural element	Elastic modulus E, MPa	Density $\rho$ , kg/m <sup>3</sup>	Poisson's ratio, $\nu$
Concrete	$0.35 \cdot 10^5$	2400	0.12
Steel reinforcement and Supporting elements	$2 \cdot 10^5$	7800	0.3
Carbon fiber sheet	$2.52 \cdot 10^5$	2000	0.28

Table 1: Physical properties of materials of the structural elements of the beam.

Numerical implementation of the model is performed using the FEM package ANSYS. Fig. 2 presents finite-element meshes used to model a concrete beam with supporting elements and steel reinforcement. To describe the deformation process, we used Solid186 (3-D 20-node solid element having 3 degrees of freedom per node and exhibiting quadratic displacement behavior) for concrete, Solid189 (3-node beam element with quadratic approximation of displacements) for reinforcement, and shell281 (8-nodes shell element with 6 degrees of freedom per node and quadratic approximation of displacements and rotation angles) for supporting plates.

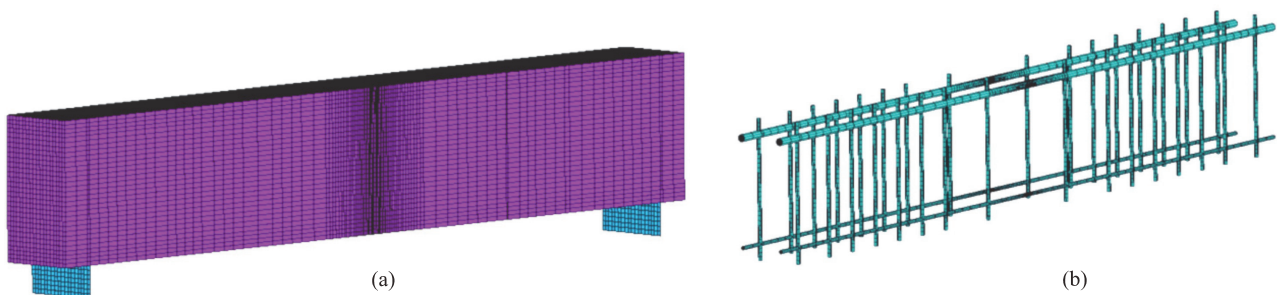


Figure 2: Finite-element mesh: concrete and supporting elements (a) and steel reinforcement (b).

The finite-element analogue of the variation equation written in matrix form is the system of ordinary linear differential equations:

$$[M]\{\ddot{U}\} + [K]\{U\} = \{f(t)\} \quad (6)$$



where  $[M]$  is the mass matrix,  $[K]$  is the rigidity matrix  $\{U\}$  and  $\{\ddot{U}\}$  are the nodal displacement and the nodal acceleration vectors, and  $\{f(t)\}$  is the external force vector.

## VARIATION OF NATURAL FREQUENCIES DUE TO CRACK INITIATION

The matrix equation for eigenmodes and eigenfrequencies of reinforced concrete beam obtained from (6) has the form

$$([K] - \omega^2 [M])\{\phi\} = 0 \quad (7)$$

where  $\{\phi\}$  is the vector specifying an eigenmode, and  $\lambda = \omega^2$  is the eigenvalue equal to the squared circular eigenfrequency. The solution of system (7) determines the set of eigenmodes  $\phi_i$  and eigenfrequencies  $\lambda_i$  ( $i = 1, 2, \dots, N$ ), where  $N$  is the order of symmetric positive definite rigidity and mass matrices.

The crack initiation affects the rigidity of the originally intact beam and, as a consequence, changes eigenfrequencies and eigenmodes. For a quantitative description of these changes, we introduce small perturbations of the stiffness matrix, eigenfrequencies and eigenmode in the form

$$[K] = [K^o] + [K^*], [M] = [M^o], \lambda_i = \lambda_i^o + \lambda_i^*, \{\phi\}_i = \{\phi^o\}_i + \{\phi^*\}_i \quad (8)$$

All variables with superscript ‘ $o$ ’ correspond to the beam without the crack, and the variables with superscript ‘ $*$ ’ determine the value of perturbation due to the crack appearance. If we substitute (8) into (7) and linearize the obtained expression with respect to the perturbation, then, after simple transformations, we get the formula

$$\lambda_i^* = \lambda_i^o \frac{\{\phi^o\}_i^T [K^*] \{\phi^o\}_i}{\{\phi^o\}_i^T [K^o] \{\phi^o\}_i} \quad (9)$$

This relation allows assessment of variations in the  $i$ -th unperturbed mode  $\{\phi^o\}_i$  and the frequency  $\lambda_i^o$  at small perturbation of the rigidity matrix  $[K^*]$ . The quantity  $\lambda_i^*$  is called here the sensitivity parameter of the  $i$ -th eigenfrequency to crack formation. A comparative analysis of the values of  $\lambda_i^*$  shows the eigenfrequencies of the available frequency spectrum, which demonstrate the strongest response to the prescribed perturbation of the rigidity matrix.

Information on these most sensitive eigenfrequencies and on the distribution of corresponding vibration forms over the surface of the beam allows us to determine the location, direction, and duration of the external action required to effectively initiate this oscillation and to find a point on the beam, at which the registration of vibration parameters will be most effective. The spectral analysis of measured vibration parameter (displacement, velocity, acceleration) ensures the possibility of assessing crack nucleation in the originally projected point or its lack.

Analysis of the spectral properties of the reinforced concrete beam having the crack of 10 mm depth and 1 mm width in its central section, showed that there are four natural frequencies in the range of 0 – 5 kHz exhibiting the greatest response to the occurrence of such a crack [21]. They are eigenfrequencies No 14 (2072 kHz) and 23 (3897 kHz), corresponding to the bending modes, and eigenfrequencies No 16 (2298 kHz) and 23 (3845 kHz), corresponding to the torsion modes. Fig. 3 shows the local areas to which the load is applied in order to excite bending and torsion vibrations, and the positions of sensors (accelerometers) capable to register these oscillations.

The solution of the initial boundary value problem modeling the vibrations in reinforced concrete beam caused by the impact impulse applied at the selected point can provide information on displacements and accelerations of arbitrary part of the structure.

Fig. 4 shows the Fourier vibroacceleration image at the sensor location point in two forms: as a diagram illustrating the frequency spectrum of vibroaccelerations (a) and as a grey scale image where different shades of grey show the intensity of the signal of prescribed frequency (b). These results were found for the beam having a crack with a depth of 10 mm and width of 1 mm.

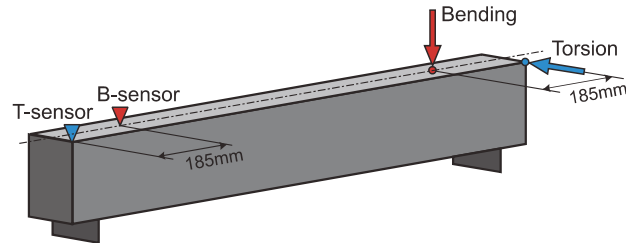


Figure 3: Scheme of local application of pulse load and the location of the accelerometer.

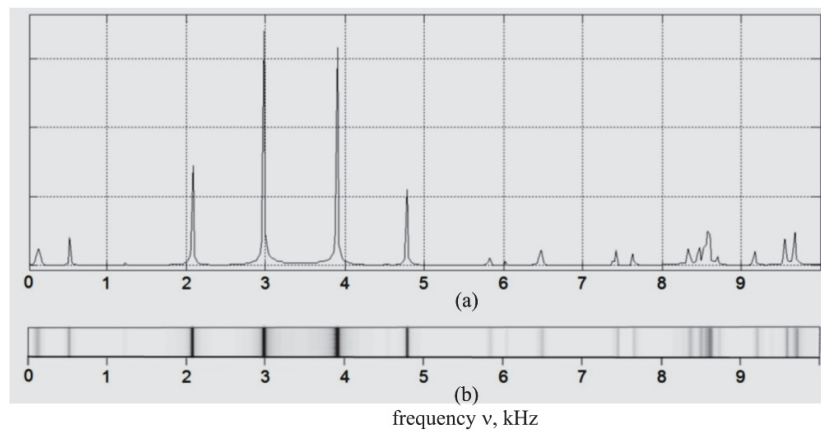


Figure 4: Fourier image of vibroacceleration: as a graph (a) and as a tone distribution (b).

By solving a series of analogous problems, in which the crack depth varies from 0 to 180 mm (the crack propagating through the entire cross-section of the beam), we have obtained a set of grey-scale images, which allowed us to get a pattern of changes in eigenfrequencies with crack extension. The results are shown in Fig. 5. The dark lines in these graphs correspond to the natural frequencies. Lines 1–4 with the greatest intensity correspond to frequencies that give the most intense signal in the Fourier image (lines 1 and 3 correspond to eigenfrequencies No 14 and 23, lines 2 and 4 – to eigenfrequencies No 16 and 24). The figure shows that as the crack depth increases, the eigenfrequencies reduce.

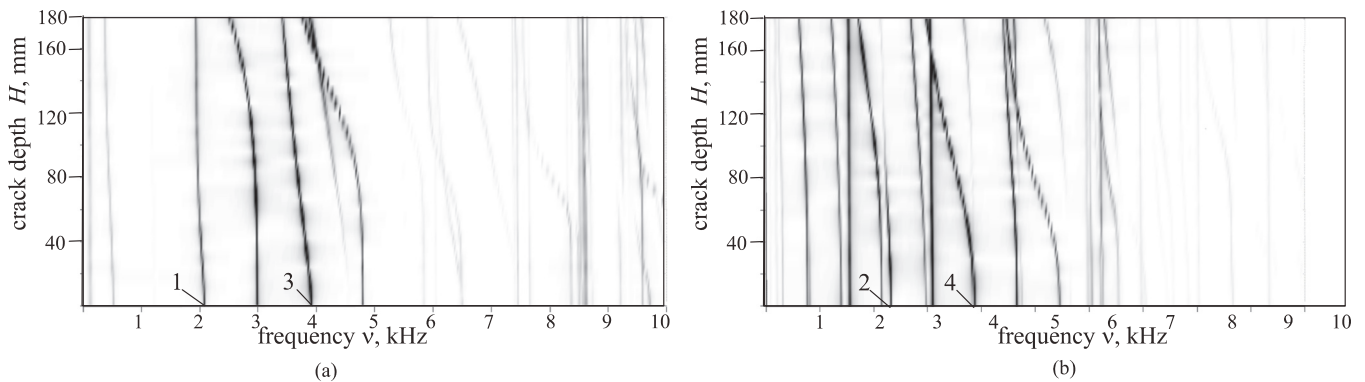


Figure 5: Changes in eigenfrequencies caused by crack propagation: bending vibration mode (a) and torsion vibration modes (b).

## EXPERIMENT

In our experiments, we used a set-up specially designed for sequential quasistatic four-point loading of a reinforced beam to initiate crack nucleation in concrete. During the experiment the beams were subjected to additional impulse loading at each loading stage.

Mathematical modeling of the vibration process allowed us to calculate the parameters necessary to provide eigenmodes exhibiting the strongest response to nucleation and evolution of cracks. Piezoelectric transducers were employed to register the vibrations. Simultaneously, visible cracks on the side surface of the beam were registered.

Tone images based on the Fourier analysis of vibrorecords were obtained from vibroacceleration measurements for each quasistatic loading step. A set of these images corresponding to increasing bending moments was used to get two-dimensional tone images in coordinates: frequency and number of the loading stage (or an appropriate bending moment).

Fig. 6(a) presents the diagrams illustrating the changes in eigenfrequencies pertaining to the bending eigenmodes, and Fig. 6(b) shows patterns of visible cracks observed at appropriate loading stages. In the diagrams, the lines corresponding to eigenfrequencies are clearly visible so that one can trace the changes in eigenfrequencies as the load increases. It is seen that before the appearance of the first crack, eigenfrequencies remain almost unchanged. The first crack with the opening width of 0.05 mm occurs at the bending moment of 4.4 kNm. At that instant, the active nucleation of many cracks began in concrete. In the tone image, this stage is witnessed by a sharp reduction in eigenfrequencies. For three identified eigenfrequencies, 2069, 3904, 4798 Hz, the measured eigenfrequency changes in the interval from the start of loading until the propagation of cracks through the entire cross section of the beam are, respectively, 7.2, 13.7, and 18.7% (Tab. 2).

By solving a series of problems of vibrations of a reinforced beam with a crack propagating through its central cross-section with increasing bending moment, we obtained theoretically the changes in eigenfrequencies. Tab. 2 shows the calculated changes in the eigenfrequencies of a beam having a crack extending through the entire cross-section (corresponding bending moment 5.0 kNm). As can be seen from the table, the experimentally determined changes in eigenfrequencies associated with cracking in concrete agree well with the results of numerical simulation.

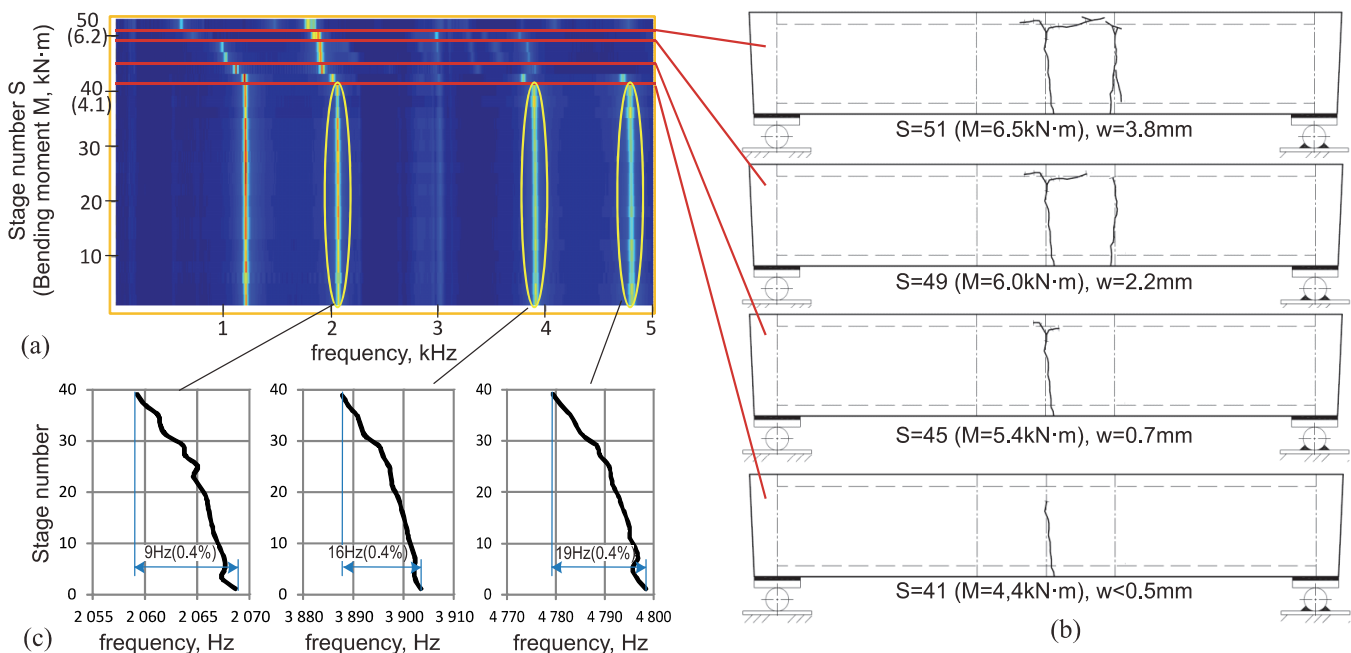


Figure 6: Changing in eigenfrequencies, corresponding bending vibration modes (a) and observed pattern of cracks (b).

A detailed study of the eigenfrequency diagram shows that at the initial stage of deformation, when no visible changes are present in concrete, the changes in eigenfrequencies have already started, yet constituting no more than 0.5% of their original value (Fig. 6(c)). Accordingly, we can identify two characteristic stages in the process of loading. At the first stage, the nonconservative deformation process begins. The signs of this process cannot be observed visually, but if we have a recording apparatus with sufficient sensitivity, they can be well recorded. The second stage is characterized by active

cracking reflecting by a sharp decrease in eigenfrequencies. It is of importance that the moment of transition from one stage to another is very well registered, because it suggests that the phase of active cracking starts.

$\nu$ , kHz	Experiment:	Simulation:
	$\Delta\nu$ , Hz ( $\Delta\nu/\nu$ , %)	$\Delta\nu$ , Hz ( $\Delta\nu/\nu$ , %)
2.069	148 (7.2)	109 (5.3)
3.904	534 (13.7)	489 (12.5)
4.798	898 (18.7)	1022 (21.4)

Table 2: Changing in eigenfrequencies at the instant of significant opening of the first crack (step 43,  $M=5.0$  kNm).

The strengthening of reinforced concrete structures with carbon fiber reinforced polymers (CFRP) is currently extensively used. The developed method of vibration diagnostics turns out to be a promising tool to analyze the deformation behavior of a concrete beam reinforced with carbon fiber plastic and to evaluate the effectiveness of this way of strengthening concrete structures.

We tested the beams strengthened with carbon fiber sheet SikaWrap-230 of 40 mm width and 0.13 mm thickness (See also the paper by *I.N. Shardakov, A.A. Bykov, A.P. Shestakov* in the present issue). A series of physical experiments were carried out to explore the spectrum of eigenfrequencies of the beam strengthened prior loading. During stepwise increasing quasistatic loading in combination with additional impulse loading, the grey-scale Fourier images were obtained (Fig. 7(a)). It is seen that a sharp change in eigenfrequencies corresponding to the formation of first visible cracks is associated with the bending moment  $M = 5.2$  kNm; the limiting state accompanied by the rupture of the CFRP sheet is achieved at  $M^* = 10.4$  kNm. Both values are essentially higher than the relevant values obtained for the unstrengthened beam.

Tab. 3 presents data showing changes in three selected eigenfrequencies registered at successive loading stages (Fig. 7). The bending moment  $M^*$  refers to the instant when the rupture of the strengthening layer takes place. The loading stages prior to the onset of first cracks are accompanied by slight changes in eigenfrequencies ( $\sim 0,6\%$ ). The nucleation of cracks causes an abrupt change in eigenfrequencies, which reaches at the instant of the rupture of CFRP about 60% of their initial values.

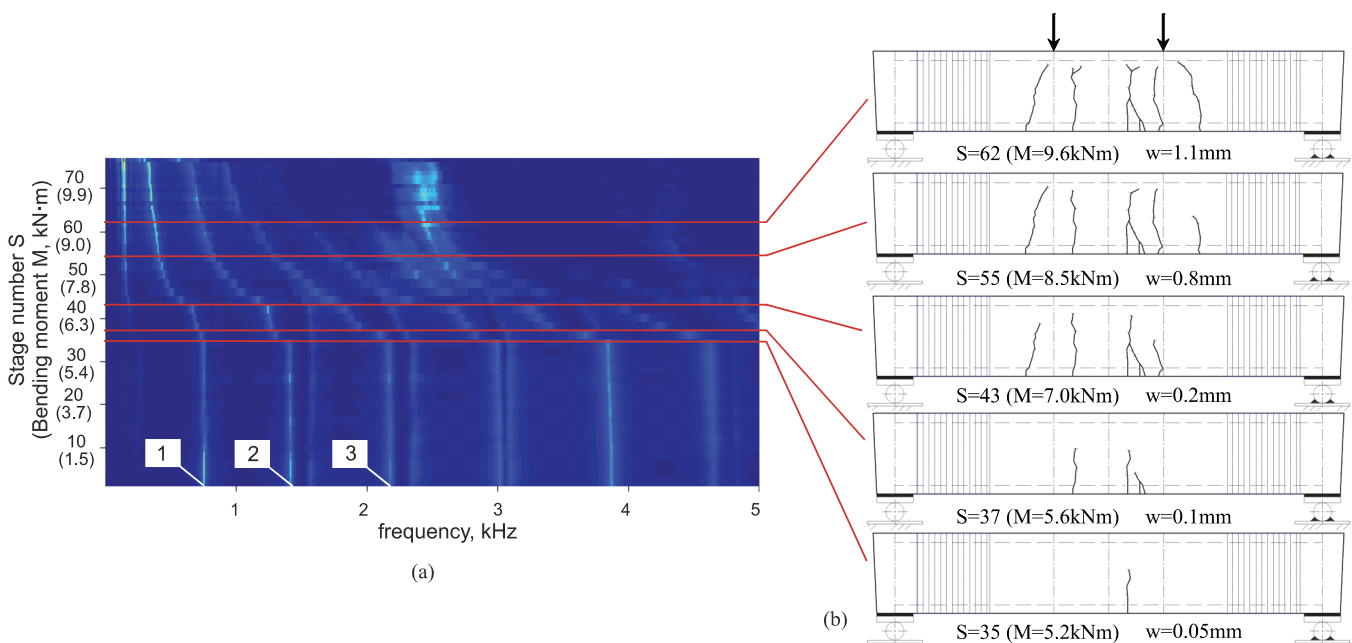


Figure 7: Changing in eigenfrequencies for the beam preliminary strengthened with the CFRP sheet (a) and observed pattern of cracks (b).



$n$	$\nu$ , kHz	before 1-st crack $M < 0.56M^*$	1-st crack $M = 0.56M^*$	cracks $M = 0.8M^*$	numerous cracks $M = M^*$	rapture of CFRP sheet
1	0.751	0.6	2.7	45.8	55.8	60.5
2	1.413	0.7	8.0	41.5	54.0	60.5
3	2.173	0.6	3.3	35.0	x	x

Table 3: Relative change in eigenfrequencies  $\Delta\nu/\nu$  (%) in the preliminary reinforced beam.

The diagram of changes in eigenfrequencies reflects the processes taking place in the beam during its repair and restoring at some intermediate loading stage (Fig. 8). The restoration procedure carried out directly under the load and consisted of the injection of cracks with the low-viscous epoxy material and gluing carbon fiber sheet to the stretched beam surface. In the loading range from 0 to 4.5 kNm, the eigenfrequencies remained practically the same, and their values reduced sharply at the onset of formation of first visible crack ( $M = 5.7\text{kNm}$ ). In the diagram, one can observe the "restoring" of eigenfrequencies after the procedure of crack treatment: they are recovered almost to their original values, which are kept over the load range from 5.7 to 7.2 kNm. A further increase in the bending moment leads to the nucleation of new generation cracks (Fig. 8(b), light lines) and therefore to new reducing in eigenfrequencies. A total loss of the bearing capacity of the beam occurs at the instant of rapture of the CFRP sheet at the bending moment of 10.4 kNm. Thus, the diagram of eigenfrequencies enables one to visualize the sharp changes in eigenfrequencies at the instant of nucleation of both primary and secondary cracks in concrete, and to identify the stage characterized by a full loss of the bearing capacity of the beam.

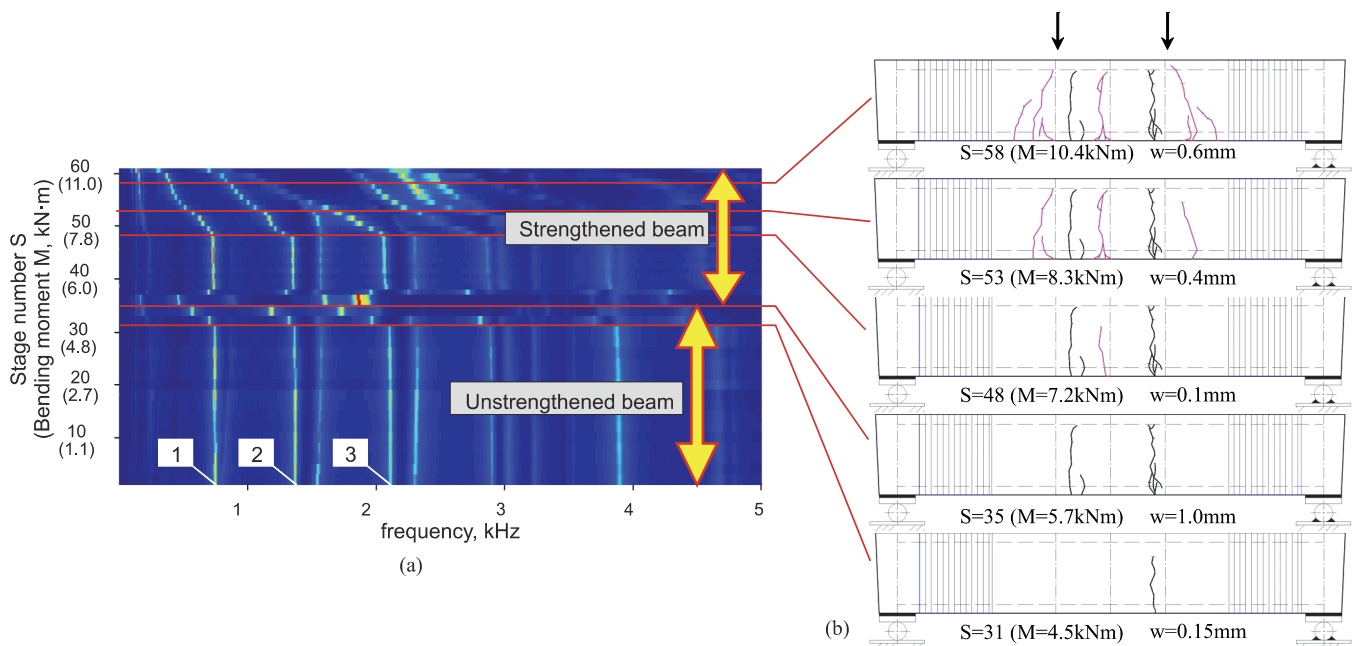


Figure 8: Changes in eigenfrequencies for the beam strengthened with the CFRP sheet under the load (a) and the observed pattern of cracks (b).

$n$	$\nu$ , kHz	before 1-st crack $M < 0.56M^*$	1-st crack (I generation) $M = 0.44M^*$	1-mm crack $M = 0.53M^*$	after treatment $M = 0.53M^*$	1-st crack (II generation) $M = 0.67M^*$	cracks $M = 0.8M^*$	numerous cracks $M = M^*$	rapture of CFRP sheet
1	0.746	0.4	6.0	38.6	1.9	3.7	36.9	50.5	58.1
2	1.367	0.6	3.5	35.8	1.2	6.9	26.8	41.0	48.7
3	2.109	0.4	6.9	24.3	2.0	3.5	26.7	x	x

Table 4: Relative change in eigenfrequencies  $\Delta\nu/\nu$  (%) of the beam reinforced under the loading.

Based on the diagram given Fig. 9, the values of loading at which first cracks occur in concrete are compared with the limiting values. As a limiting condition, we assume a state when multiple cracks spread over the entire cross-section of the beam, and the bearing capacity of the beam is completely ensured by the steel reinforcement (in the experiment it is the bending moment equal to 6.5 kNm). The experiment proves that, from the appearance of the first cracks until the loss of the bearing capacity (4.4 kNm to 6.5 kNm), the beam continues to be functional despite of nucleation of new cracks and propagation of existing ones. In this case, the beam has the strength reserve constituting  $\sim 32\%$  of the limiting load. The beam reinforced with the CFRP sheet also retains its workability after the onset of first cracks. The bending moment of the preliminary strengthened beam corresponding to the full rupture of the sheet exceeds the load at which the occurrence of first cracks has been registered by  $\sim 45\%$ , and the bending moment of the beam strengthened during the loading by  $\sim 56\%$ . The analysis of the diagram confirms the validity of procedures aimed at strengthening a beam under the loading. The effectiveness of such reinforcement techniques is competitive with that of the procedures for preliminary strengthening of beams with a composite material. Summing up, our experiment clearly demonstrates that crack formation in concrete is not a critical factor affecting the loss of bearing capacity by a reinforced concrete beam.

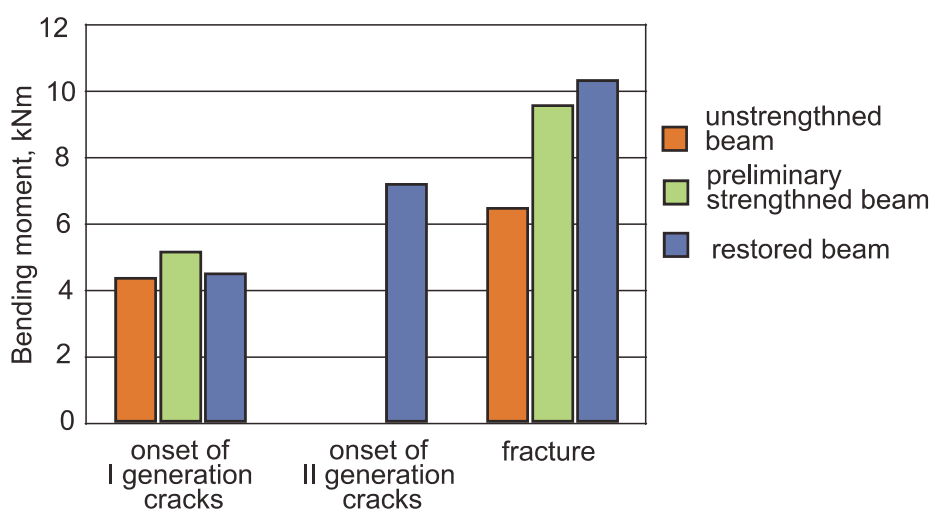


Figure 9: Critical values of the bending moment.

## CONCLUSION

Based on the results of experimental and theoretical studies, we conclude that vibration diagnostics of reinforced concrete structures is an effective tool for early detection, assessment, and monitoring of cracking. The real-time vibration analysis gives a great deal of information about the level of cracking and the residual life of the concrete structure. The developed method of vibration diagnostics enables one to assess the degree of efficiency of measures for the restoration and strengthening of the structure. The obtained data provide a general algorithm for creating and performing procedures for vibration diagnostics of cracking in reinforced concrete structures. The algorithm consists of the following steps:

- 1) Based on mathematical modeling, the deformation state of the structure is assessed by using information on actual loading conditions. The most probable locations of cracks are predicted.
- 2) A series of numerical experiments are carried out to simulate vibrations in the structure. Eigenmodes and eigenfrequencies are analyzed for the entire structure and the structure having cracks in the predicted areas.
- 3) Using numerical simulation results, the parameters of vibrodiagnostic testing are specified, namely:
  - technical characteristics of vibration sensors that provide registration of vibrations in a predetermined frequency range with a required precision;
  - vibration sensors location points;
  - position and duration of external impact, ensuring excitation of vibrations with required natural frequencies.
- 4) Rational scheme for strengthening a reinforced concrete structure based on numerical simulation data is developed.
- 5) Block diagram for the system of vibration diagnostics of cracking in reinforced concrete structures is elaborated.



## ACKNOWLEDGMENT

This research was supported by the Russian Science Foundation, project No. 14-29- 00172.

## REFERENCES

- [1] Raghavan, A., Cesnik, C.E.S., *Shock and Vibration Digest*, 39 (2007) 91-116.
- [2] Grimberg, R., Premel, D., Savin, A., Bihan, Y. Le, Placko, Y. D., Eddy current holography evaluation of delamination in carbon-epoxy composites, *Insight*, 34 (2001) 260-264.
- [3] Maldague, X.P.V., *Nondestructive Evaluation of Materials by Infrared Thermography*, Springer, London, (2011).
- [4] Ermolov, I.N., Aleshin, N.P., Potapov, A.I., *Acoustic Testing Methods*. Moscow, Vysshaya Shkola, (1991) (in Russian).
- [5] Chikhunov, D., *Methods and Devices for Nondestructive Testing of Physical Properties of Concretes*, *Stroit.Inzhener* 3(2005) 55–59 (in Russian).
- [6] Verma, K., Bhadauria, S.S., Akhtar, S., Review of non destructive testing methods for condition monitoring of concrete structures, *Journal of Construction Engineering* (2013). <http://dx.doi.org/10.1155/2013/834572>.
- [7] Rahmani, T., Kiani, B., Bakhshi, M., Shekarchizadeh, M., Application of different fibers to reduce plastic shrinkage cracking of concrete, *7th RILEM International Conference on Cracking in Pavements*, (2012) 635-642.
- [8] Cao, M., Ren, Q., Qiao, P., Nondestructive assessment of reinforced concrete structures based on fractal damage characteristic factors, *Journal of Engineering Mechanics*, 132 (2006) 924-931.
- [9] Adams, D., Farrar, C., Classifying linear and nonlinear structural damage using frequency domain arx models, *Structural Health Monitoring*, 1 (2002) 185–201.
- [10] Doebling, S., Farrar, C., Prime, M., Shevitz, D., *Damage identification and health monitoring of structural and mechanical systems from changes in their vibration characteristics: a literature review*, Los Alamos National Laboratory, Los Alamos, New Mexico, (1996).
- [11] Fan, W., Qiao, P., Vibration-based damage identification methods: a review and comparative study, *Structural Health Monitoring*, 10 (2011) 83-111. DOI: 10.1177/1475921710365419.
- [12] Wang, L., Chan, T.H.T., Review of vibration-based damage detection and condition assessment of bridge structures using structural health monitoring, *Proc. 2-nd infrastructure theme postgraduate conference*. Queensland University of Technology, (2009).
- [13] Cawley, P., Adams, R.D., The location of defects in structures from measurements of natural frequencies, *Journal of Strain Analysis*, 14 (1997) 49-57.
- [14] West, W.M., Illustration of the use of modal assurance criterion to detect structural changes in an orbiter test specimen, *Proc. 4th International Modal Analysis Conference*, Union College, (1986).
- [15] Pandey, A.K., Biswas, M., Samman, M.M., Damage detection from changes in curvature mode shapes, *Journal of Sound and Vibration*, 145 (1991) 321–332. doi:10.1016/0022-460X(91)90595-B
- [16] Stubbs, N., Kim, J.T., Damage detection in offshore jacket structures from limited modal information, *International Journal of Offshore and Polar Engineering* 5(1995) 58-66.
- [17] Aktan, A.E., Lee, K.L., Chuntavan, C., Aksel, T., Modal testing for structural identification and condition assessment of constructed facilities, *Proc. 12th International Modal Analysis Conference*, (1994) 462–468.
- [18] Spagnoli, A., Carpinteri, A., Ferretti, D., Vantadori, S., An experimental investigation on the quasi-brittle fracture of marble rocks, *Fatigue and Fracture of Engineering Materials and Structures*, 39 (2016) 956-958. doi:10.1111/file.12429.
- [19] Montanari, L., Spagnoli, A., Basu, B., Broderick, B., On the effect of spatial sampling in damage detection of cracked beams by continuous wavelet transform, *Journal of Sound and Vibration*, 345 (2015) 233-249. doi: 10.1016/j.jsv.2015.01.048.
- [20] Montanari, L., Basu, B., Spagnoli, A., Broderick, B.M., A padding method to reduce edge effects for enhanced damage identification using wavelet analysis, *Mechanical Systems and Signal Processing*, 52-53 (2015) 264-277. doi: 10.1016/j.ymssp.2014.06.014.



- [21] Bykov, A.A., Matveenko, V.P., Serovaev, G.S., Shardakov, I.N., Shestakov, A.P., Mathematical modeling of vibration processes in reinforced concrete structures for setting up crack initiation monitoring, *Mechanics of Solids*, 50 (2015) 160–170.
- [22] Bykov, A.A., Matveenko, V.P., Serovaev, G.S., Shardakov, I.N., Shestakov, A.P., Analysis of the influence of dynamic phenomena on the fracture of a reinforced concrete beam under quasistatic loading (Computations and experiment), *Mechanics of Solids*, 50 (2015) 118–129.
- [23] Lurie, A.I., *The Theory of Elasticity*, Moscow, Nauka (1970) (in Russian).